ASIAN BULLETIN OF BIG DATA MANAGMENT
Vol. 4. Issue 2 (2024)
https://doi.org/ 10.62019/abbdm.v4i02.11.

ASIAN BULLETIN OF BIG DATA MANAGEMENT
http://abbdm.com/
ISSN (Print): 2959-0795
ISSN (online): 2959-0809

Spatiotemporal Drought Assessment in Ningxia Autonomous Region: A Machine Learning and Remote Sensing Approach

Muhammad Awais, Zakria Zaheen, Zainab Fatima*, Muhammad Shahwar, Naveed Jan, Shahzad Ali

Chronicle

Article history

Received: April 20, 2024
Received in the revised format: May 3, 2024
Accepted: May 15, 2024
Available online: May 17, 2024

Muhammad Awais, Zakria Zaheen & Muhammad Shahwar are currently affiliated with College of Computer Science and Technology, Qingdao University, Qingdao 266071, China.
Email: akkhan8801@gmail.com
Email: zakriazaheen10@gmail.com
Email: shahwarmughal10@gmail.com

Zainab Fatima is currently affiliated with the Institute of Geo-Information and Earth Observation, Arid Agriculture University, Rawalpindi Punjab 46000, Pakistan.
Email: syedazainab7662@gmail.com

Naveed Jan is currently affiliated with the Department of Information Engineering Technology, University of Technology Nowshera, 24100, KPK, Pakistan.
Email: naveed.jan@uotnowshera.edu.pk

Shahzad Ali is currently affiliated with the College of life sciences, Zhejiang normal university, Jinhua, China.
Email: shahzadali330@aup.edu.pk

Corresponding Author*

Abstract

Drought represents a significant disaster that directly impacts the economic and ecological welfare of any nation it afflicts. This study focused on the climatic anomalies of drought over the Ningxia Hui autonomous region in northwest China over the last two decades. The study employed an in-depth machine learning model, which incorporated drought indices, thus leading to a data-informed analysis of Ningxia drought patterns. The study accomplished this by using MODIS satellite data products available for vegetation and moisture monitoring. The MOD09GA, MOD11A2, and MCD43A4 data streams were loaded into Google Earth Engine as factors to develop a time-series dataset of vegetation indices. Indices are Normalized Difference Vegetation Index (NDVI), Enhanced Vegetation Index (EVI), and Land Surface Temperature (LST) measurements are taken into account. Data on temperature, precipitation, and evapotranspiration was compiled for the period from 2003 to 2023 and calculated standardized indices on pixel level for the whole Ningxia region to develop the Standardized Precipitation Index (SPI), Keetch-Byram Drought Index (KBDI), and Standardized Precipitation-Evapotranspiration Index (The study results indicated that SPI fell significantly from the year 2003 to 2023, from 0.7 to -0.3. The SPEI plummeted from 0.5 to -0.2 during the observed time frame. KBDI also went up, through 581.33 in 2003 and 681.091 in 2023, showing deterioration of aridity and drying of the soil. The conclusion of this study focuses on the deterioration of drought conditions in the Ningxia region in the last 20 years.

Keywords: Drought, Machine Learning, EVI, SPI, SPEI, KBDI.

INTRODUCTION

Drought is a cyclic natural calamity that impacts agricultural output, water reserves, ecology, and socio-economic progress (Cheng et al., 2023). It can result in significant declines in crop production, strain water resources, raise the likelihood of fires, and result in substantial financial losses (Xu et al., 2024). Given the growing threat of drought caused by climate change, it is essential to be aware of past trends and weaknesses to develop effective measures for adapting to and mitigating its impacts (Gosh et al., 2024). The Ningxia Hui Autonomous Region in northwest China is susceptible to droughts due to its arid climate, elevated temperatures, and limited yearly rainfall (Kafy et al., 2023). This study examines the drought patterns in Ningxia from 2003 to 2023 by utilizing satellite remote sensing data and climatic records (Tyagi et al., 2022). Machine learning techniques, such as regression trees and random forests, are employed to create models that capture the connections between remote sensing inputs and the intensity of drought (Mardian et al., 2023). Drought disasters, defined as prolonged periods of substantially reduced precipitation, have wide-ranging effects on the environment, agriculture, and human societies (Zhang et al., 2023). They are closely connected to the constantly changing dynamics of our climate system, and their occurrence and intensity are affected by changes in atmospheric conditions and consistent weather patterns (Mohammed et al., 2024). Droughts, resulting from increasing temperatures and continuous decreases in precipitation levels, result in the decline of soil moisture, decreasing water resources, and lower agricultural productivity. These droughts can worsen vulnerabilities in areas with dry climates or limited access to water reservoirs, producing significant challenges for food security, livelihoods, and the availability of safe drinking water. The ongoing climate change increases the frequency and intensity of drought occurrences, rendering them more frequent and severe (Gallear et al., 2024). Understanding the interaction between drought and climate is essential for efficient catastrophe management and adaptive solutions. This comprehension aids in reducing the effects of droughts, guaranteeing sustainable farming methods, and enhancing community resilience (Alkaraki et al., 2023).

The Standardized Precipitation Index (SPI) and the Standardized Precipitation Evapotranspiration Index (SPEI) are now essential tools for global drought monitoring agencies and decision-makers. The World Meteorological Organization (WMO) acknowledged the pressing need for integrated drought management, recognizing that droughts encompass various aspects, including climate, water resources, and society (Yue et al., 2023). The recommendations on Integrated Drought Management (IDM) provide a comprehensive framework for effectively managing the impacts of drought (Zhang et al., 2023). They emphasize the proactive collaboration of many sectors, stakeholders, and institutions (Foroumandi et al., 2023). The study aims to examine the spatiotemporal occurrence of drought disasters in the Ningxia Hui Autonomous Region of China over the past two decades. This will be achieved using MODIS remote sensing, climate data, and a machine learning methodology. The study seeks to analyze drought's temporal and spatial fluctuations, evaluate its effects on agriculture, and ascertain the specific attributes of drought in the area. The project will utilize multi-temporal MODIS data to examine spatiotemporal fluctuations in dryness in the area and evaluate the precision of the machine learning method in forecasting drought.

MATERIALS AND METHODS

Study Area

The Ningxia Hui Autonomous Region in far northwestern Asia of China has a very huge area of 66,400 square kilometers. It must be additionally millions of people being there. There is an aridity situation, with less rain and higher evaporation. The ordinary temperature is namely higher. The mean annual precipitation which is weary (varying from) 200 to 700 mm, is majorly distributed from the months of July to September when the East Asian monsoon rains arrive, making up to 80 and 60%, respectively. The average temperature of Ningxia ranges from -10°C to 25°C. The region falls within the North Temperate Zone with a continental monsoon climate, and its capital city is Yinchuan

(Pandya et al., 2023). The Yellow River flows through Ningxia. By providing an important water source for irrigation and hydropower but also contributing to problems like flooding, soil erosion, and desertification.

Study Area Map

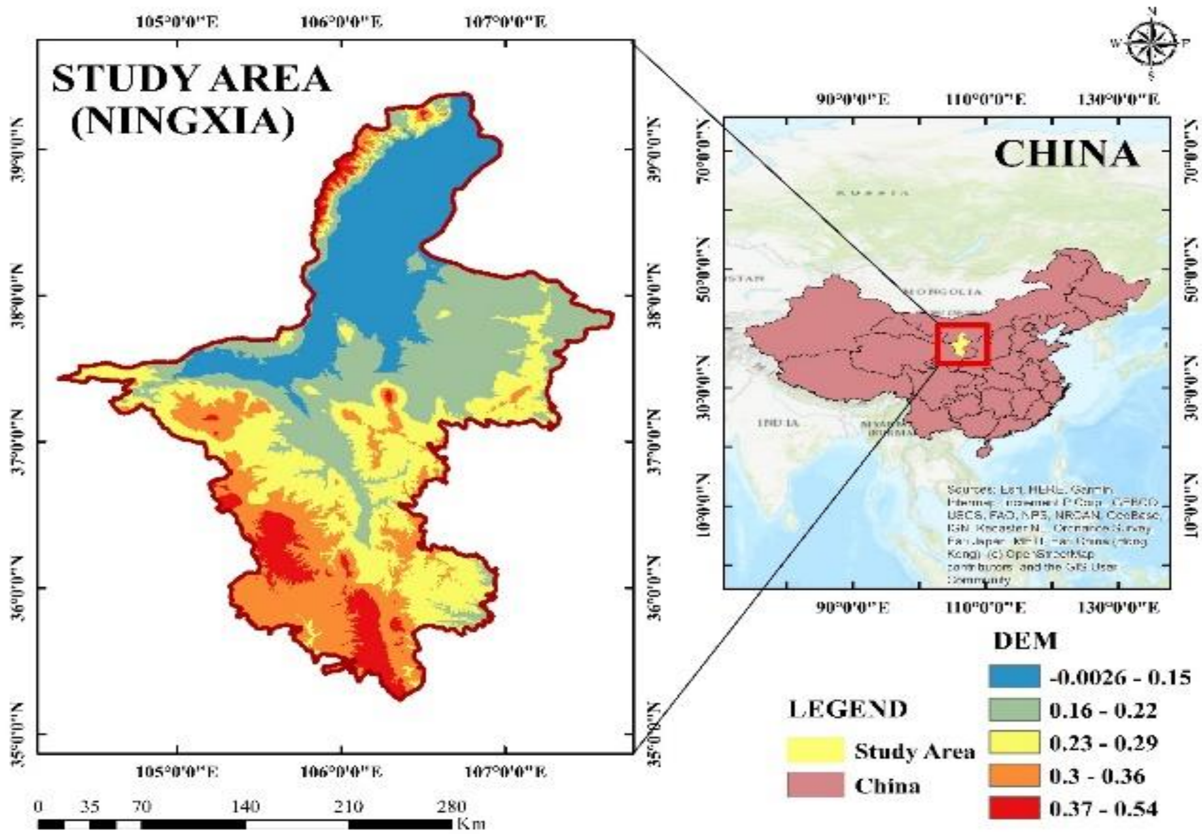

Figure 1.
Study Area Map

Datasets

This study benefited from the diversification of satellite platforms and types of remote sensors to gather data at various points over a 20-year span. The key data sources were MOD09GA, MOD11A2, and MCD43A4 products, all of which are based on the Moderate Resolution Imaging Spectroradiometer (MODIS) reducing system (Speer et al., 2024). The data from MODIS gives a range of spatial resolution covering 500 meters to 1200 kilometers, helping in capturing the detailed and broad features across the study area. Also, the study area is combined with climate data from the Climate Data repository and boundary information from the DIVA-GIS database (Chen et al., 2023). Integration of climate data from the two-decade period allowed the researchers to investigate long-term trends and patterns that might be significant to the understudied area. The boundary data, on the other hand, facilitated the delineation of the study region and the identification of key geographical features of interest (Prodhan et al., 2022). The data collection spanned three distinct years, 2003, 2022, and 2023, which would be the years selected as they give us an overall temporal perspective on the matter, thereby allowing us to see the underlying trends as well as the changes over time (Shahfahad et al., 2024). The channels incorporated in this study, namely Earth Explorer, Earth Engine, Climate Data, and DIVA-GIS, have established names and hard-earned reputations. Thus, the overall credibility and authority of the data within the study are guaranteed.

SPEI: Standardized Precipitation Evapotranspiration Index, KBDI: Keetch-Byram drought index.

Table 2.
Summary of vegetation and drought indices.

Product	Data Used	Spatial Resolution	Temporal Resolution	Formula
NDVI	MOD09GA	500m	Daily	$=\frac{NIR-Red}{NIR+Red}$
LST	MOD11A2	1200*1200km	8-day	$=DN \times 0.02-273.15$
EVI	MCD43A4	463.313m	16-Day	$=2.5*\frac{NIR-Red}{(NIR+C1*Red-C2*BLUE+L)}$
SPI	CHIRPS precipitation	-	Monthly	$=\frac{X-Xm}{\sigma}$
SPEI	CSIC/SPEI/2_8	1°	24 Month	$=W-\frac{c0+\mathrm{c1W}+\mathrm{c2}W^2}{1+d1W+d2W^2+d3W^3}$
KBDI	WTLAB/KBDI/v1	-	Daily	$=\mathrm{Q}+\frac{(800-Q).(0.968.e^{0.0486.T}-8.30).\Delta t}{1+10.88.e^{0.0486.T}}.10^{-3}$

Note: NDVI: Normalized Difference Vegetation Index, LST: Land Surface Temperature, EVI: Enhanced Vegetation Index, SPI: Standardized Precipitation Index, SPEI: Standardized Precipitation Evapotranspiration Index, KBDI: Keetch-Byram drought index Table 3 summarizes agricultural drought disaster models using machine learning models (MLMs). MLMs are utilized for drought prediction based on available data.

Table 3
Agricultural drought prediction summary using machine learning models (MLMs).

Model	Data type	Predictor variables	Response variable	Forecasting lead time	Outcome
CART, and SVM	MODIS	EVI, NDVI, LST	SPEI	Seasonal	Increased drought area prediction
SVM	Meteorological data	Slope, aspect, elevation, annual precipitation	SPI	-	Agricultural drought prediction
Cubist	MODIS, TRMM and climate data	NDVI, EVI, LST	SPI	Seasonal	Severe Drought Index Mapping
SVM	Soil Moisture	LST, ET, EVI, precipitation, NDVI	SPEI and crop yield	12-months	Drought severity distribution maps

CART and SVM models predict SPEI annually, Cubist models predict SPI on a seasonal basis, and LSTM models predict SPEI on a 12-month basis using various data types like soil moisture, LST, ET, EVI, precipitation, and NDVI (Han et al., 2021).

Figure 2.
Methodology Flowchart

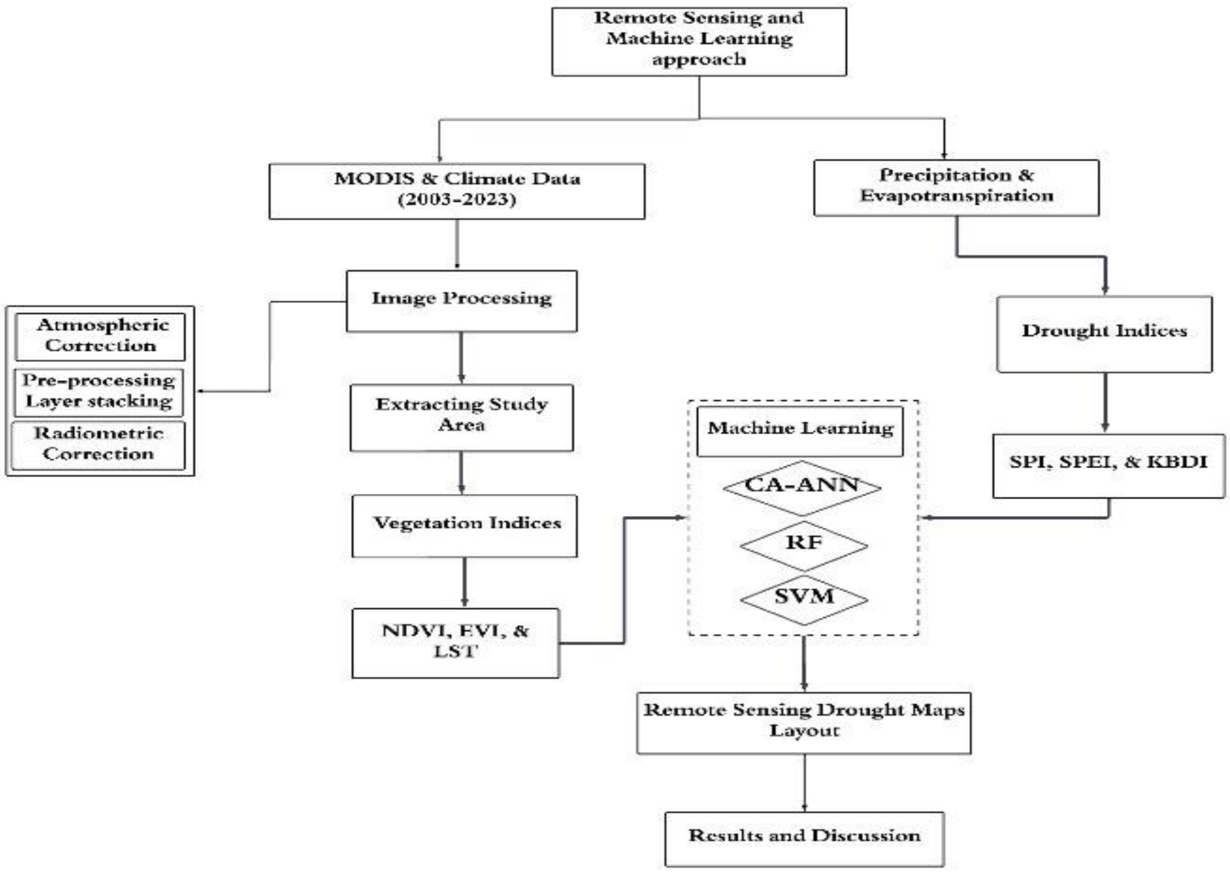

PROCESSING AND METHODS

Remote Sensing Indices for Drought

The Normalized Difference Vegetation Index (NDVI) is a remote sensing metric used to quantify the presence of healthy green vegetation within a given region (Li et al., 2021). The calculation is performed using a machine learning technique that combines the reflectance coefficients of near-infrared and red light emitted by the Earth's surface. The research area in Ningxia was used to perform NDVI analysis on Google Earth Engine using MODIS/MOD09GA surface reflectance variables. The MOD09GA.006 Terra Surface Reflectance Daily Global 1km and 500m dataset was utilized to retrieve the NDVI. The Normalized Difference Vegetation Index (NDVI) varies between -1.0 to 1.0 (Mardian et al., 2023).

$$NDVI = \frac{NIR - Red}{NIR + Red}$$

The Enhanced Vegetation Index (EVI) is an satellite metric that calculates vegetation coverage via interpretation of infrared, red, and blue spectrum signals coming from the surface of the Earth (Karbasi et al., 2023). A research of this form, in Ningxia, China, is carried using Google Earth Engine. The EVI extends from -1 to 1, with the higher positive value meaning that vegetation is more abundant. Cooling planet earth is the major purpose for MODIS Combined 16-Day EVI product. This product derived from MODIS/006/MCD43A4 surface reflectance composites and has a resolution of 1 pixel which is 463.313 meters (Lalika et al., 2024).

$$EVI = 2.5 * \frac{NIR - Red}{(NIR + C1 * Red - C2 * BLUE + L)}$$

Land Surface Temperature (LST) is an essential parameter for monitoring the Earth's surface temperature and its changes over time. The MODIS/061/MOD11A2 dataset was used to measure Land Surface Temperature (LST) on the Google Earth Engine in Ningxia (Hao et al., 2023). It provides an average 8-day LST in a 1200 x 1200-kilometer grid, allowing for the tracking of variations in land surface temperature and the consequences of climate change (Adnan et al., 2023).

$$LST = DN \times 0.02 - 273.15$$

Machine learning algorithms have the ability to detect patterns in data, which leads to progressive enhancement of software performance (Zhang et al., 2023). The Standardized Precipitation statistic (SPI) is a commonly employed statistic that is utilized to describe agricultural drought across different time periods (Sharafi et al., 2023). The research area in Ningxia utilized the CHIRPS precipitation dataset to conduct estimates of the Standardized Precipitation Index (SPI). The script was run in Google Earth Engine and consisted of two separate calculations: one for the "common" SPI (n-month) and the other based on MODIS capture dates. Spectral precipitation index (SPI) can be utilized to observe variations in precipitation and investigate the influence of climate change on Earth's precipitation patterns (Wang et al., 2023).

$$SPI = \frac{X - Xm}{\sigma}$$

X = precipitation for the station, Xm = Mean Precipitation, σ = Standardized deviation.

Table 4.
Classification of SPI

SPI Category	Value
Less than -2	Extremely dry
Between -1.5 & -2	Severely dry
Between -1 & -1.5	Dry
Between -0.5 & -1	Moderately dry
Between 0.5 & -0.5	Normal
Between 0.5 & 1	Wet
Between 1 & 1.5	Moderately wet
Between 1.5 & 2	Severely wet
More than 2	Extremely wet

The Standardized Precipitation Evapotranspiration Index (SPEI) is a drought index that relies on data regarding precipitation and evapotranspiration (Sadiq et al., 2023). The study conducted in Ningxia utilized the CSIC/SPEI/2_8 dataset, which offers global maps and data of the Standardized Precipitation-Evapotranspiration Index (SPEI) at a spatial resolution of 1° for the entire Earth (Archite et al., 2023). The study spanned a duration of 24 months. The dataset was analyzed, and drought conditions were monitored over time using machine learning methods. The SPEI parameters consist of the sum of monthly precipitation and monthly potential evapotranspiration, which is determined using the Thornthwaite equation. The calculation of the Standardized Precipitation

Evapotranspiration Index (SPEI) includes subtracting reference evapotranspiration from precipitation in order to provide a more accurate indicator of the severity of drought (He et al., 2023).

$$SPEI = W - \frac{c_0 + c_1 W + c_2 W^2}{1 + d_1 W + d_2 W^2 + d_3 W^3}$$

Where:

$$W = \sqrt{-2\ln(P)} \text{ for P} \leq 0.5$$

P = probability of exceeding a determined D value, p=1-f(x);

When P > 0.5, p=1-P, constants are:

$c_0 = 2.515517$	$d_1 = 1.432788$
$c_1 = 0.802853$	$d_2 = 0.189269$
$c_2 = 0.010328$	$d_3 = 0.001308$

Table 5.
Classification of SPEI

SPEI Category	SPEI Value
Extremely wet	More than 2.00
Very wet	1.50 to 1.99
Moderately wet	1.00 to 1.49
Near Normal	-0.99 to 0.99
Moderately dry	-1.00 to -1.49
Severely dry	-1.50 to -1.99
Extremely dry	Less than -2.00

The Keetch-Byram drought index (KBDI) is a method utilized to assess the deficiency of soil moisture by considering measures of daily precipitation and temperature (Feng et al., 2019). It was utilized in the research area of Ningxia to establish a consistent reference scale for assessing the dryness of soil and duff layers. The indicator exhibits a positive correlation with high temperatures and is not influenced by the absence of rainfall. The scale ranges from 0 (no moisture deficit) to 800 (extreme drought). The KBDI is widely used for drought monitoring for national weather forecasts and wildfire prevention, especially in regions with rain-fed crops (Rui et al., 2023).

$$\text{KBDI} = \text{Q} + \frac{(800 - Q).(0.968.e^{0.0486.T} - 8.30).\Delta t}{1 + 10.88.e^{0.0486.T}}.10^{-3}$$

Q, which represents the previous day's KBDI adjusted by the net rainfall in inches per hundred (cf. details below); T, the air temperature in degrees Fahrenheit; Δt, the time increment (typically one day); and P, signifying the mean annual precipitation in inches. When it comes to temperature, the maximum air temperature, or the dry-bulb temperature observed at the time of the essential measurement, should be used as the relevant input.

$$Q = KBDI_{t-1} - \text{P}net_t.100$$

$$\mathrm{P}net_t = \max\,[0, P_t\ - \max\,(0, P_{\mathrm{lim}} - \sum_{i=1}^{rr-1} P_{\mathrm{t-i}}\,)$$

With "rr" denoting the count of consecutive days on which rain has occurred.

RESULTS

Normalized Difference Vegetation Index (NDVI)

The NDVI performed on MODIS data from 2003 to 2023 on the Ningxia, China study area shows a general decrease in vegetation over time. Machine learning was used to analyze and predict the spatiotemporal dynamics of vegetation in Ningxia, China. By applying machine learning algorithms to the MODIS, patterns, and trends in the vegetation changes over time were identified. Figure 3 shows that the highest NDVI

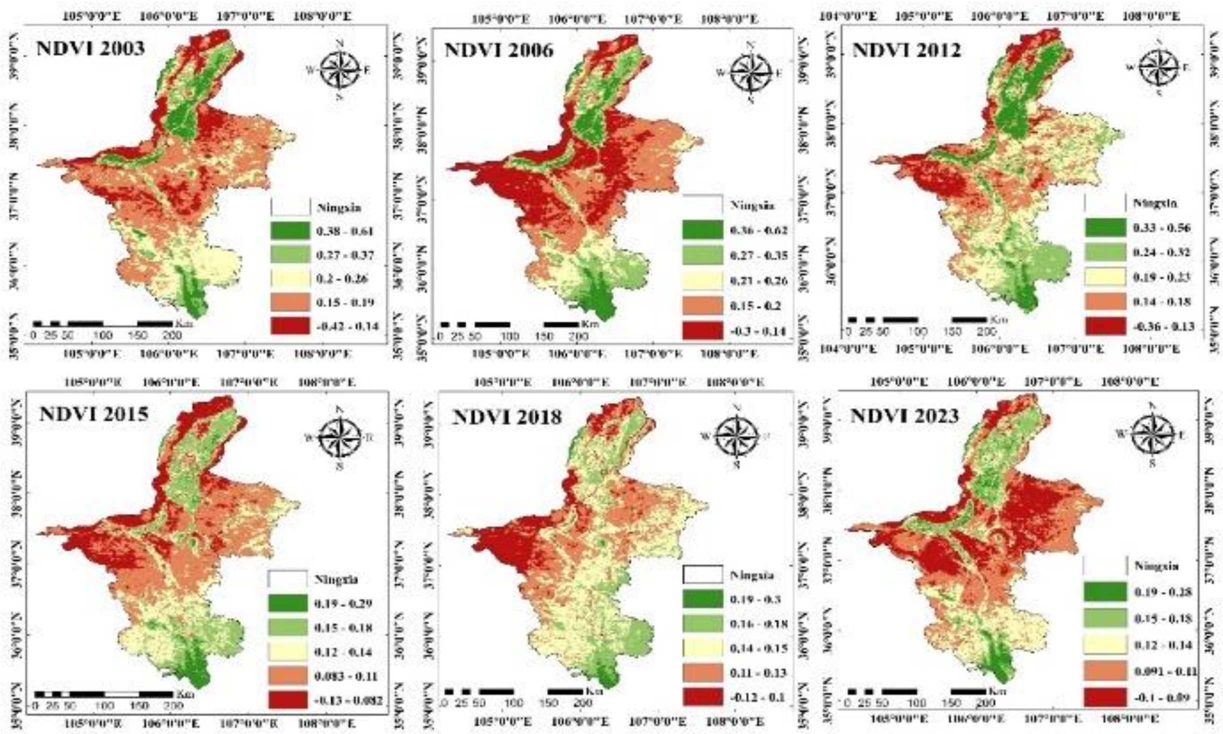

values were recorded in 2003, with a high of 0.38 and a low of -0.14. The lowest NDVI values were recorded in 2023, with a high of 0.19 and a low of -0.09. The decline in NDVI is most probably attributed to a confluence of causes, encompassing climate change, alterations in land use, and urbanization. The most significant declines in NDVI have been observed in the central and western regions of Ningxia.

Figure 3.
NDVI Map 2003-2023

Enhanced Vegetation Index EVI

The EVI was performed using Google Earth Engine using MODIS in Ningxia, China, from 2003 to 2023. Machine learning techniques have been used to monitor desertification changes in Ningxia. Figure 5 shows that the average annual soil erosion rate for Ningxia, China, from 2003 to 2023 has been increasing. The average EVI in 2003 was -0.11, while the average in 2023 was -0.09. It represents an increase of 18% over the 20 years. Climate change has led to more frequent and severe droughts, which can increase the risk of soil erosion.

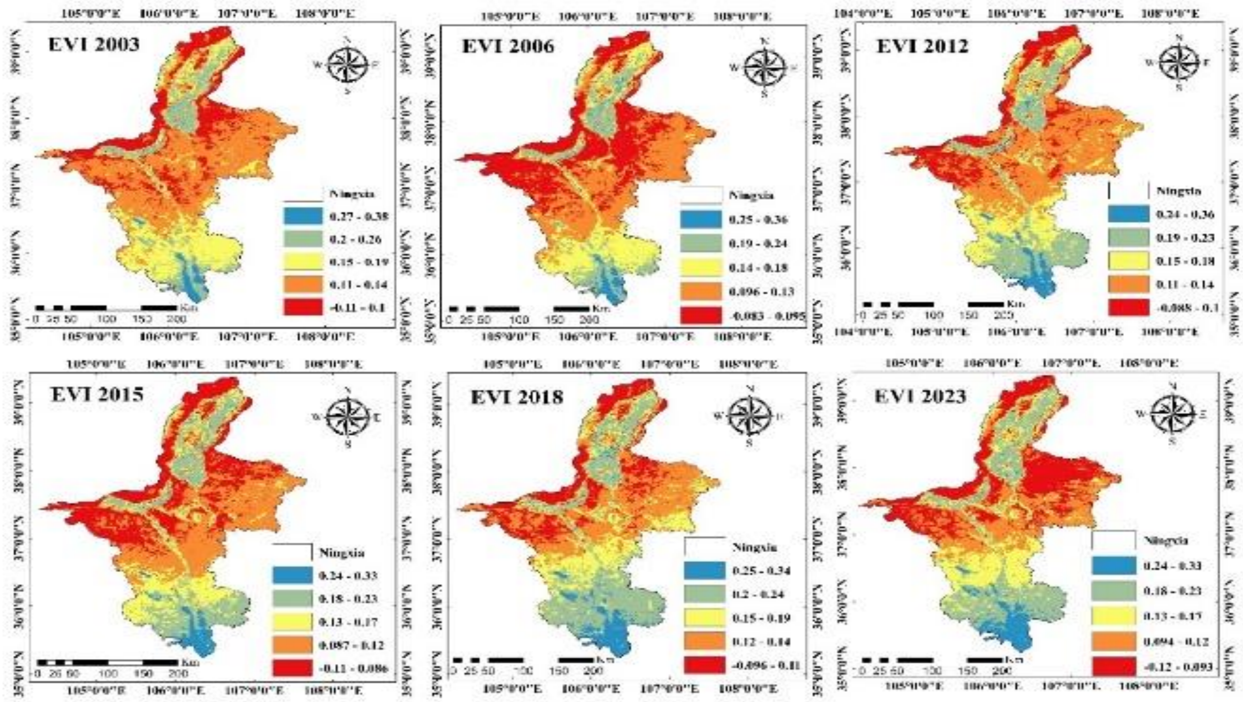

Figure 6,
EVI Map from 2003-2023

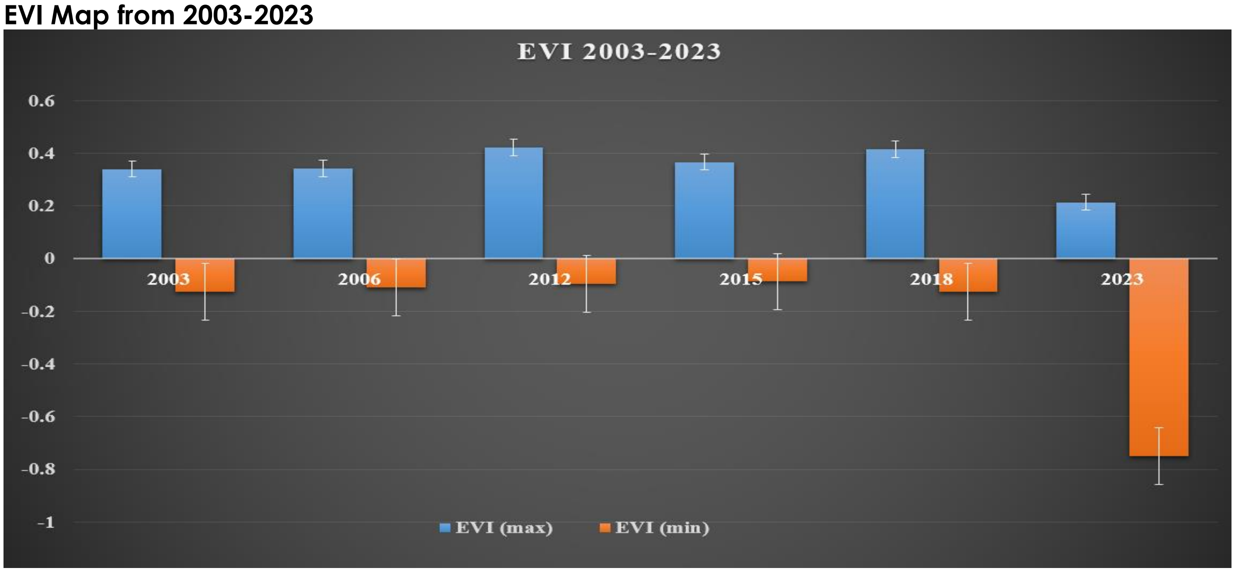

Figure 5.
EVI graph showing fluctuations in droughts from 2003-2023

Land Surface Temperature (LST)

The map in Figure 7 shows the Land Surface Temperature (LST) of Ningxia, China, from 2003 to 2023. A machine learning technique was used to integrate the GEE. Model package to estimate LST from 2003 to 2023 using data in Earth Engine and a trained model. Which were derived from MODIS data using the Google Earth Engine. The LST is in degrees Celsius, with a range of 4.6-31. LST of Ningxia has increased over time. In 2003, the average LST of Ningxia was 14.3 degrees Celsius. By 2023, the average LST of Ningxia had increased to 16.7 degrees Celsius.

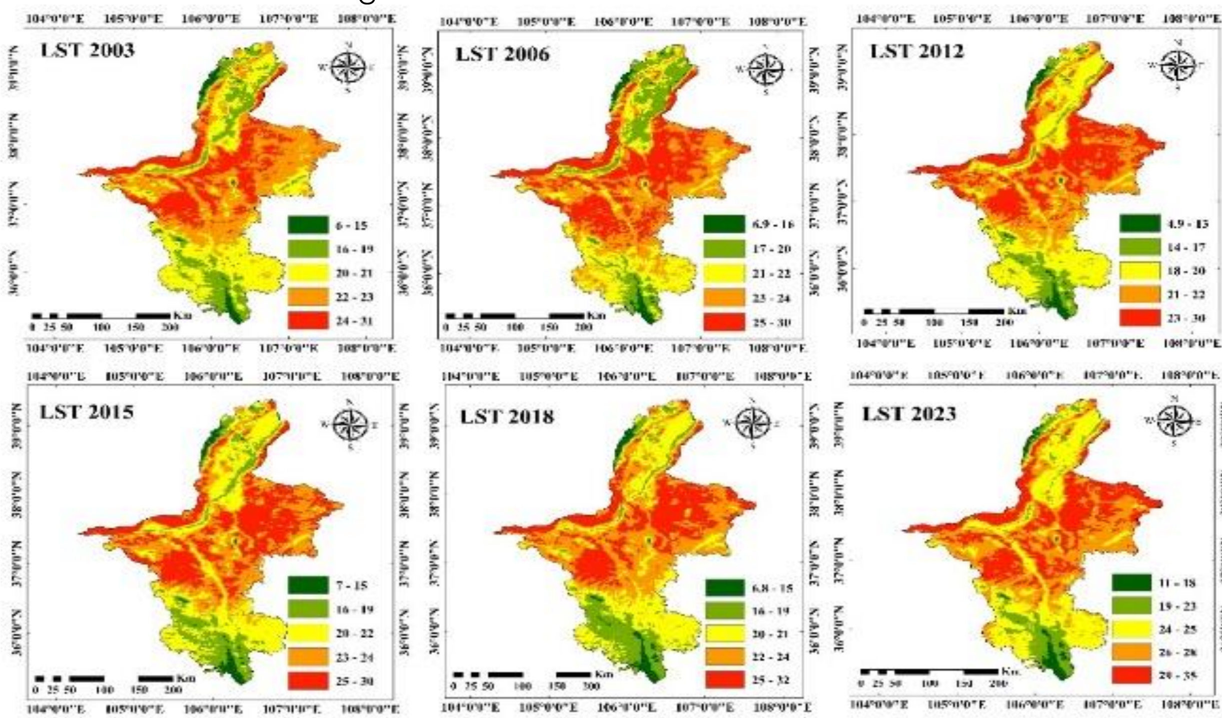

Figure 7.
LST Map from 2003-2023

Figure 8.
LST graph displaying the incline in temperature of land surface from 2003 to 2023

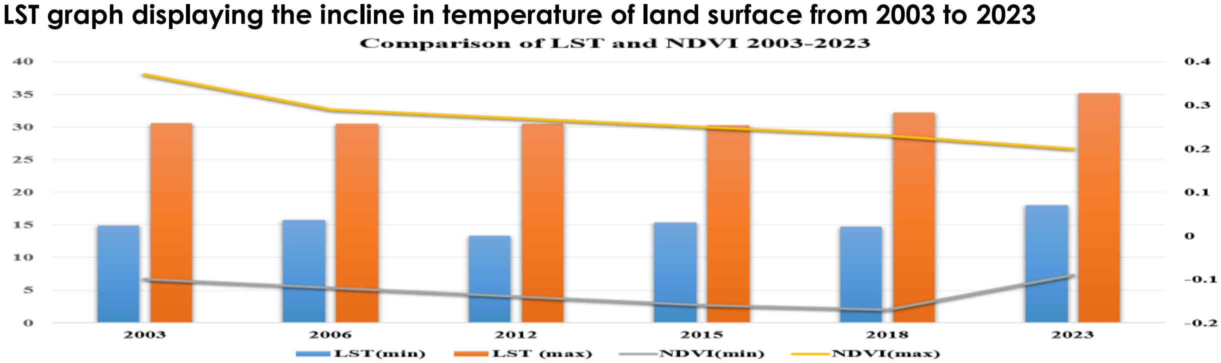

Figure 9.

Comparison graph of LST and NDVI shows the inverse relation. Land surface temperature (LST) is increasing while the Normalized Difference Vegetation Index (NDVI) is decreasing from 2003 to 2023.

Standardized Precipitation Index (SPI)

The map in Figure 10 shows that the SPI of Ningxia has fluctuated over time but has generally decreased since 2003. Machine learning technique was used to analyze the factors that contribute to the shifts in SPI. In 2003, the average SPI of Ningxia was 0.7. By 2023, the average SPI of Ningxia had decreased to -0.3. This decrease in SPI indicates that Ningxia has become drier over time. The change in the spatial distribution of SPI is likely a result of various variables, such as alterations in climatic patterns and land utilization.

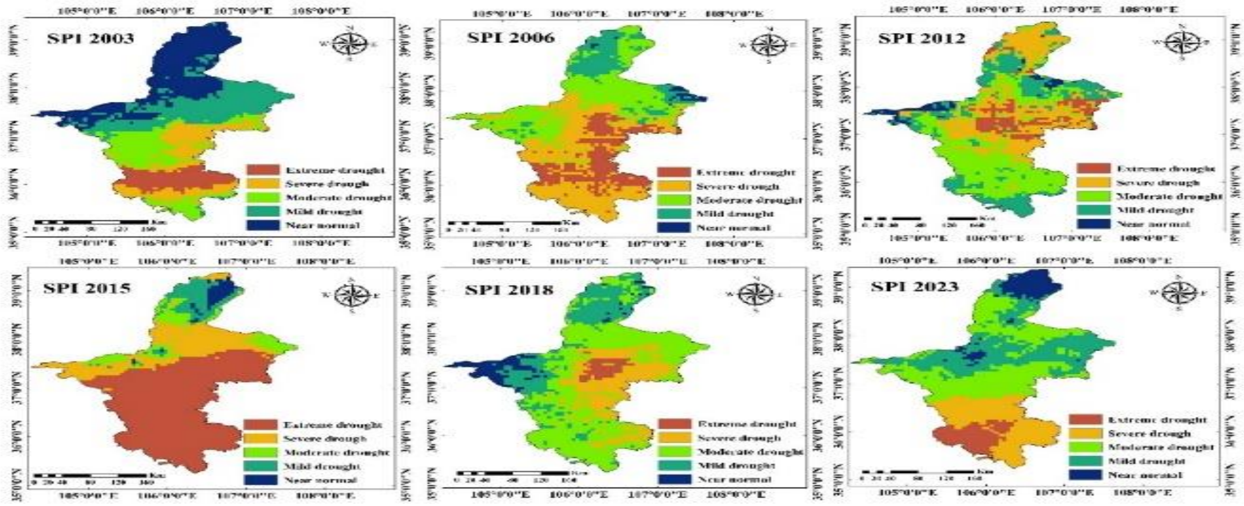

Figure 10.
SPI Maps from 2003-2023

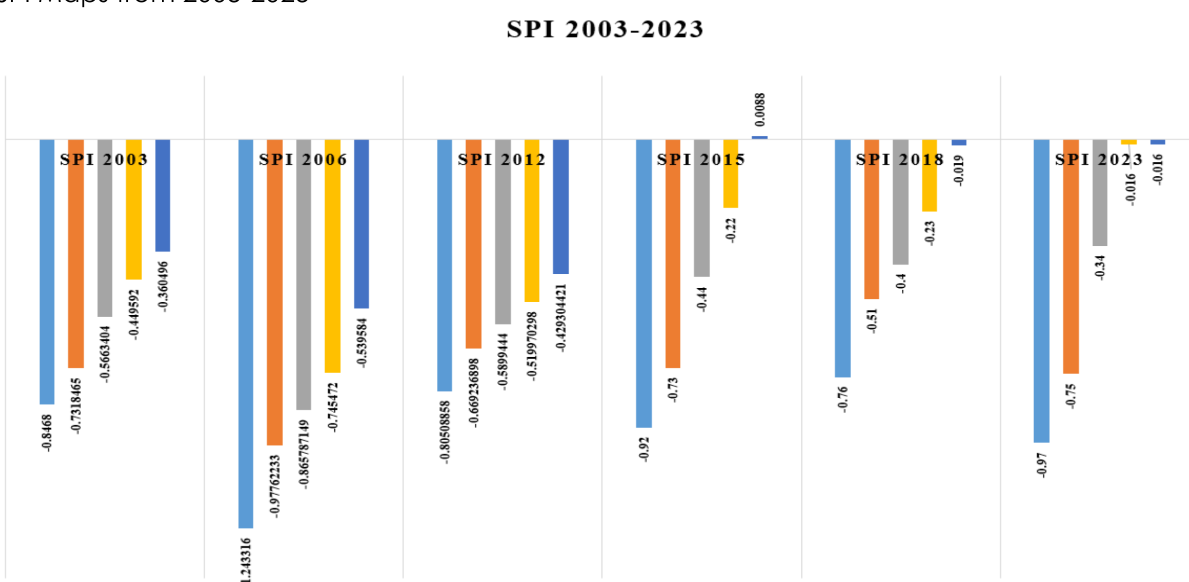

Figure 11.

The SPI graph shows an apparent reduction in moisture levels in the region between 2003 and 2023, which can be attributed to climate change, population expansion, and alterations in land utilization.

Standardized Precipitation Evapotranspiration Index (SPEI)

The SPEI was employed as an indicator to identify the likelihood of drought using machine learning algorithms implemented via the Google Earth Engine (GEE) platform. The Standardized Precipitation-Evapotranspiration Index (SPEI) in Ningxia has exhibited temporal variability, but overall, it has experienced a downward trend since 2003. The average SPEI of Ningxia in 2003 was 0.5, as depicted in Figure 12. In 2023, the average SPEI in Ningxia has declined to -0.2. The decline in SPEI suggests a progressive aridification of Ningxia.

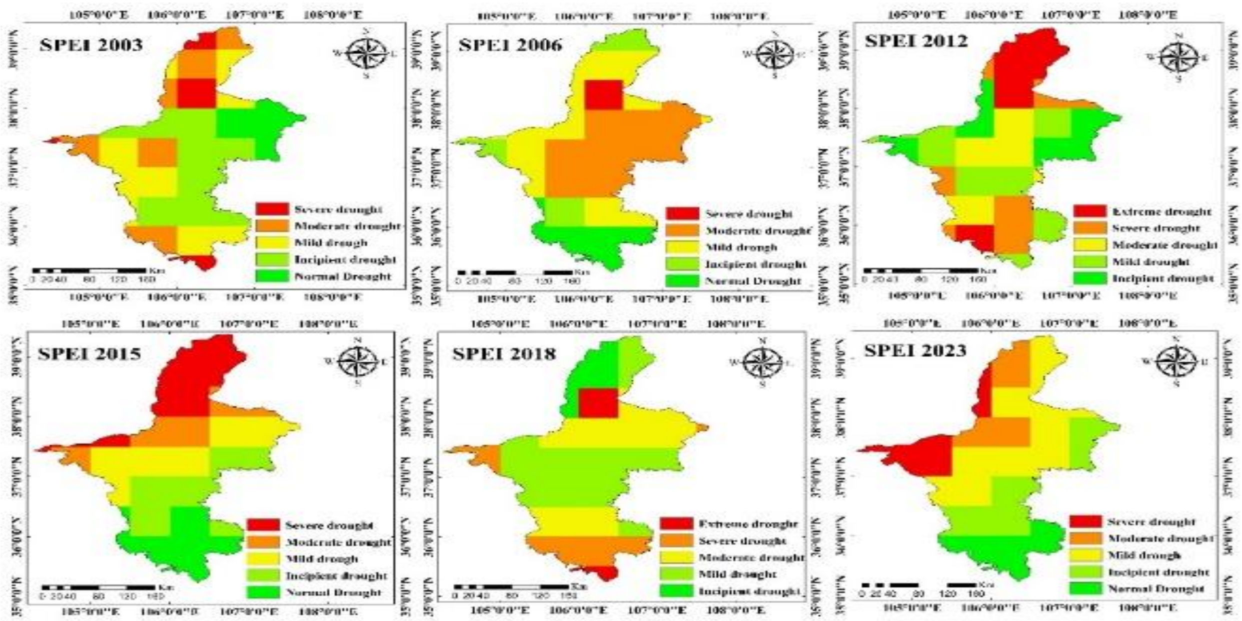

Figure 12.
SPEI Maps from 2003-2023

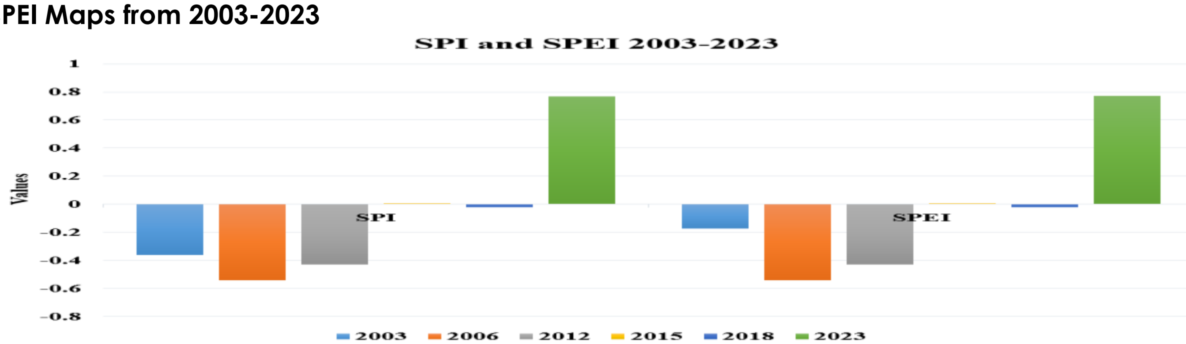

Figure 13.
The graph compares SPI and SPEI, showing a negative trend in the region, with SPEI experiencing a more severe drying trend compared to SPI.

Keetch-Byram Drought Index (KBDI)

Machine learning techniques have been employed to examine the KBDI, which is a metric used to assess dryness and the risk of wildfires. The map depicted in Figure 14 illustrates a gradual increase in Ningxia's average Keetch-Byram Drought Index (KBDI) throughout the years, rising from 581.133 in 2007 to 681.091 in 2023. This suggests a more arid climate and a heightened susceptibility to wildfires in the area. The spatial distribution of the Keetch-Byram Drought Index (KBDI) has undergone temporal changes.

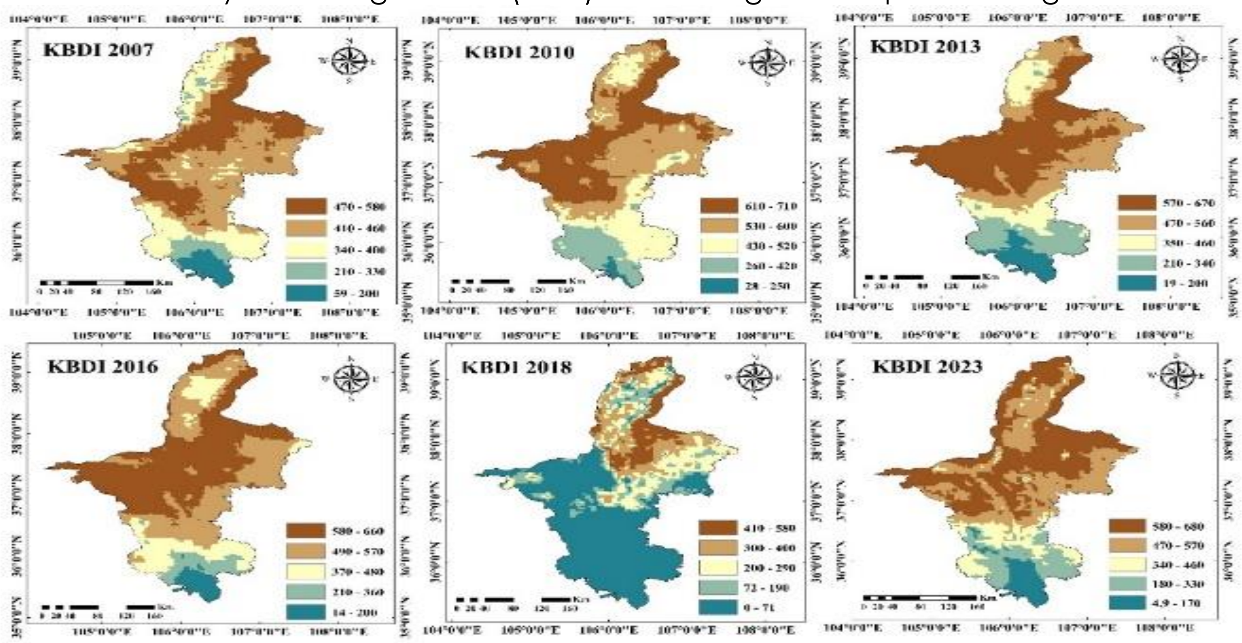

Figure 14.
KBDI Maps from 2007-2023

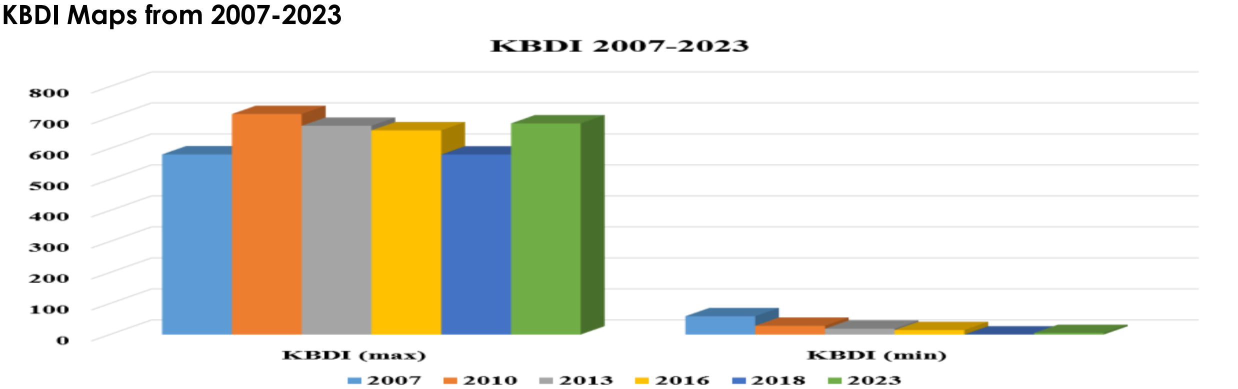

Figure 15.
The Keetch-Byram Drought Index (KBDI) graph spanning from 2007 to 2023 demonstrates an upward trend in the frequency of drought conditions in recent years.

CONCLUSION

MODIS images from 2003 and 2023 were procured and were, in turn, modified for atmospheric correction, radiometric correction, and extraction of the study area during pre-processing. LST measurement was performed using the MODIS LST algorithm. Moderate Resolution Imaging Spectroradiometer (MODIS) reflectance data was used for the calculation of vegetation indices (NDVI and EVI). Meteorological stations transmitted information about precipitation and evapotranspiration. The drought indices (SPI, KBDI, and SPEI) were computed using data on precipitation, temperature, and evapotranspiration observation. The RF model was modeled and trained to classify the drought intensity levels. The model was trained on a dataset that was a combination of drought indices and land cover data. The level of drought severity for each time scale is being determined for the years 2003 and 2023. During that survey period, drought intensity increased to the point of crisis in certain parts of the region. The Random Forest (RF) model correctly split the levels of drought severity with accuracy above 85% level. An increase of 15% and 10%, respectively, in the expanse of severe and moderate drought regions was noted from 2003 to 2023. Mild drought was also reduced by 25% in a similar time frame. The findings of this work may be applied to design solutions for drought reduction and adaptation in the Ningxia Hui Autonomous Region.

DECLARATIONS

Acknowledgement: This work was supported by the Central Guiding Local Science and Technology Development Fund of Shandong-Yellow River Basin Collaborative Science and Technology Innovation Special Project (No. YDZX2023019).

Funding: No funding body in the public, private, or nonprofit sectors provided a particular grant for this research.

Availability of data and material: In the approach, the data sources for the variables are stated.

Authors' contributions: Each author participated equally to the creation of this work.

Conflicts of Interests: The authors declare no conflict of interest.

Consent to Participate: Yes

Consent for publication and Ethical approval: Because this study does not include human or animal data, ethical approval is not required for publication. All authors have given their consent.

REFERENCE

Achite, M., Elshaboury, N., Jehanzaib, M., Vishwakarma, D. K., Pham, Q. B., Anh, D. T., ... & Elbeltagi, A. (2023). Performance of machine learning techniques for meteorological drought forecasting in the Wadi Mina Basin, Algeria. *Water*, *15*(4), 765.

Adnan, R. M., Dai, H. L., Kuriqi, A., Kisi, O., & Zounemat-Kermani, M. (2023). Improving drought modeling based on new heuristic machine learning methods. *Ain Shams Engineering Journal*, *14*(10), 102168.

Alkaraki, K. F., & Hazaymeh, K. (2023). A comprehensive remote sensing-based Agriculture Drought Condition Indicator (CADCI) using machine learning. *Environmental Challenges*, *11*, 100699.

Chen, X., Li, X., Jiang, B., Su, J., Zheng, X., & Wang, G. (2023). Prediction of spring agricultural drought using machine learning algorithms in the southern Songnen Plain, China. *Land Degradation & Development*, *34*(13), 3836-3849.

Cheng, M., Zhong, L., Ma, Y., Wang, X., Li, P., Wang, Z., & Qi, Y. (2023). A new drought monitoring index on the Tibetan Plateau based on multisource data and machine learning methods. *Remote Sensing*, *15*(2), 512.

Feng, P., Wang, B., Li Liu, D., & Yu, Q. (2019). Machine learning-based integration of remotely-sensed drought factors can improve the estimation of agricultural drought in South-Eastern Australia. *Agricultural Systems*, *173*, 303-316.

Foroumandi, E., Nourani, V., Huang, J. J., & Moradkhani, H. (2023). Drought monitoring by downscaling GRACE-derived terrestrial water storage anomalies: A deep learning approach. *Journal of Hydrology*, *616*, 128838.

Gallear, J. W., Valadares Galdos, M., Zeri, M., & Hartley, A. (2024). Application of machine learning to forecast agricultural drought impacts for large scale sub-seasonal drought monitoring in Brazil. *Natural Hazards and Earth System Sciences Discussions*, *2024*, 1-37.

Ghosh, S., Lu, J., Das, P., & Zhang, Z. (2024). Machine learning algorithms for merging satellite-based precipitation products and their application on meteorological drought monitoring over Kenya. *Climate Dynamics*, *62*(1), 141-163.

Han, H., Bai, J., Yan, J., Yang, H., & Ma, G. (2021). A combined drought monitoring index based on multi-sensor remote sensing data and machine learning. *Geocarto International*, *36*(10), 1161-1177.

Hao, R., Yan, H., & Chiang, Y. M. (2023). Forecasting the Propagation from Meteorological to Hydrological and Agricultural Drought in the Huaihe River Basin with Machine Learning Methods. *Remote Sensing*, *15*(23), 5524.

He, Q., Wang, M., Liu, K., Li, B., & Jiang, Z. (2023). Spatiotemporal analysis of meteorological drought across China based on the high-spatial-resolution multiscale SPI generated by machine learning. *Weather and Climate Extremes*, *40*, 100567.

Kafy, A. A., Bakshi, A., Saha, M., Al Faisal, A., Almulhim, A. I., Rahaman, Z. A., & Mohammad, P. (2023). Assessment and prediction of index based agricultural drought vulnerability using machine learning algorithms. *Science of The Total Environment*, *867*, 161394.

Karbasi, M., Jamei, M., Malik, A., Kisi, O., & Yaseen, Z. M. (2023). Multi-steps drought forecasting in arid and humid climate environments: Development of integrative machine learning model. *Agricultural Water Management*, *281*, 108210.

Lalika, C., Mujahid, A. U. H., James, M., & Lalika, M. C. (2024). Machine learning algorithms for the prediction of drought conditions in the Wami River sub-catchment, Tanzania. *Journal of Hydrology: Regional Studies*, *53*, 101794.

Mardian, J. (2023). *Drought Monitoring and Agricultural Risk Assessment in the Canadian Prairies Using Earth Observation and Machine Learning* (Doctoral dissertation, University of Guelph).

Mardian, J., Champagne, C., Bonsal, B., & Berg, A. (2023). A machine learning framework for predicting and understanding the Canadian drought monitor. *Water Resources Research*, *59*(8), e2022WR033847.

Mohammed, S., Arshad, S., Alsilibe, F., Moazzam, M. F. U., Bashir, B., Prodhan, F. A., ... & Harsányi, E. (2024). Utilizing machine learning and CMIP6 projections for short-term agricultural drought monitoring in central Europe (1900–2100). *Journal of Hydrology*, 130968.

Pandya, P., & Gontia, N. K. (2023). Early crop yield prediction for agricultural drought monitoring using drought indices, remote sensing, and machine learning techniques. *Journal of Water and Climate Change*, *14*(12), 4729-4746.

Prodhan, F. A., Zhang, J., Hasan, S. S., Sharma, T. P. P., & Mohana, H. P. (2022). A review of machine learning methods for drought hazard monitoring and forecasting: Current research trends, challenges, and future research directions. *Environmental modelling & software*, *149*, 105327.

Rui-xi, H. U. A. N. G., Jun-fang, Z. H. A. O., Zhi-guo, H. U. O., Hui-wen, P. E. N. G., & Hong-fei, X. I. E. (2023). Application of Deep Learning Technology in Monitoring, Forecasting and Risk Assessment of Agricultural Drought. *Chinese Journal of Agrometeorology*, *44*(10), 943.

Sadiq, M. A., Sarkar, S. K., & Raisa, S. S. (2023). Meteorological drought assessment in northern Bangladesh: A machine learning-based approach considering remote sensing indices. *Ecological Indicators*, *157*, 111233.

Shahfahad, Talukdar, S., Ghose, B., Islam, A. R. M. T., Hasanuzzaman, M., Ahmed, I. A., ... & Afzal, M. (2024). Predicting long term regional drought pattern in Northeast India using advanced statistical technique and wavelet-machine learning approach. *Modeling Earth Systems and Environment*, *10*(1), 1005-1026.

Sharafi, S., & Ghaleni, M. M. (2023). Enhancing drought monitoring and prediction in diverse climates by using composite drought indices. *Stochastic Environmental Research and Risk Assessment*, 1-21.

Speer, M., Hartigan, J., & Leslie, L. M. (2024). Machine Learning Identification of Attributes and Predictors for a Flash Drought in Eastern Australia. *Climate*, *12*(4), 49.

Tyagi, S., Zhang, X., Saraswat, D., Sahany, S., Mishra, S. K., & Niyogi, D. (2022). Flash drought: Review of concept, prediction and the potential for machine learning, deep learning methods. *Earth's Future*, *10*(11), e2022EF002723.

Wang, L., Zhang, Y., Chen, X., Liu, Y., Wang, S., & Wang, L. (2023). Ensemble learning based on remote sensing data for monitoring agricultural drought in major winter wheat-producing areas of China. *Progress in Physical Geography: Earth and Environment*, 03091333231188814.

Xu, X., Chen, F., Wang, B., Harrison, M. T., Chen, Y., Liu, K., ... & Hu, K. (2024). Unleashing the power of machine learning and remote sensing for robust seasonal drought monitoring: A stacking ensemble approach. *Journal of Hydrology*, *634*, 131102.

Yue, H., Yu, X., Liu, Y., & Wang, X. (2023). The Construction and Migration of a Multi-source Integrated Drought Index Based on Different Machine Learning. *Water Resources Management*, *37*(15), 5989-6004.

Zhang, B., Salem, F. K. A., Hayes, M. J., Smith, K. H., Tadesse, T., & Wardlow, B. D. (2023). Explainable machine learning for the prediction and assessment of complex drought impacts. *Science of The Total Environment*, *898*, 165509.

Zhang, J., Ding, J., Wang, J., Lin, H., Han, L., Li, X., & Liu, J. (2023). Remote sensing drought factor integration based on machine learning can improve the estimation of drought in arid and semi-arid regions. *Theoretical and Applied Climatology*, *151*(3), 1753-1770.

Zhang, Y., Xie, D., Tian, W., Zhao, H., Geng, S., Lu, H., ... & Choy Lim Kam Sian, K. T. (2023). Construction of an integrated drought monitoring model based on deep learning algorithms. *Remote Sensing*, *15*(3), 667.